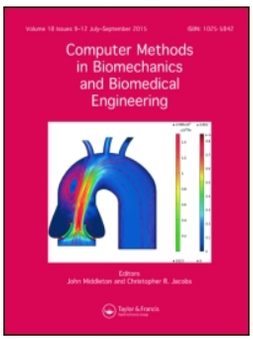

Computer Methods in Biomechanics and Biomedical Engineering

ISSN: 1025-5842 (Print) 1476-8259 (Online) Journal homepage: http://www.tandfonline.com/loi/gcmb20

A novel method for prediction of dynamic smiling expressions after orthodontic treatment: a case report

Fanfan Dai, Yangjing Li, Gui Chen, Si Chen & Tianmin Xu

To cite this article: Fanfan Dai, Yangjing Li, Gui Chen, Si Chen & Tianmin Xu (2016) A novel method for prediction of dynamic smiling expressions after orthodontic treatment: a case report, Computer Methods in Biomechanics and Biomedical Engineering, 19:3, 340-346, DOI: 10.1080/10255842.2015.1025767

To link to this article: http://dx.doi.org/10.1080/10255842.2015.1025767

Computer Methods in Biomechanics and Biomedical Engineering, 2016
Vol. 19, No. 3, 340–346, http://dx.doi.org/10.1080/10255842.2015.1025767

Taylor & Francis
Taylor & Francis Group

A novel method for prediction of dynamic smiling expressions after orthodontic treatment: a case report

Fanfan Dai[a], Yangjing Li[b], Gui Chen[a], Si Chen[a]* and Tianmin Xu[a]*

[a]*Department of Orthodontics, Peking University School and Hospital of Stomatology, 100081 Beijing, P.R. China;* [b]*Center for BioMed-X Research, Academy for Advanced Interdisciplinary Studies, Peking University, 100871 Beijing, P.R. China*

(*Received 14 September 2014; accepted 2 March 2015*)

Smile esthetics has become increasingly important for orthodontic patients, thus prediction of post-treatment smile is necessary for a perfect treatment plan. In this study, with a combination of three-dimensional craniofacial data from the cone beam computed tomography and color-encoded structured light system, a novel method for smile prediction was proposed based on facial expression transfer, in which dynamic facial expression was interpreted as a matrix of facial depth changes. Data extracted from the pre-treatment smile expression record were applied to the post-treatment static model to realize expression transfer. Therefore smile esthetics of the patient after treatment could be evaluated in pre-treatment planning procedure. The positive and negative mean values of error for prediction accuracy were 0.9 and -1.1 mm respectively, with the standard deviation of ± 1.5 mm, which is clinically acceptable. Further studies would be conducted to reduce the prediction error from both the static and dynamic sides as well as to explore automatically combined prediction from the two sides.

Keywords: cone beam computed tomography; structured light system; expression transfer; smile prediction; orthodontic treatment

1. Introduction

Patients seeking orthodontic treatment usually have two major concerns, teeth alignment and facial esthetics. Although the former could be accurately controlled by orthodontists, the later may hard to be predicted due to the complexity of facial soft tissues. Since a predicted facial esthetic result was a keen anticipation of both patients and doctors, many studies were done aiming to solve this problem. Previous studies on sagittal profile changes using 2D methods obtained various ratios of lip position and teeth movement, which were difficult to be applied to an individual patient (Roos 1977; Hillesund et al. 1978; Waldman 1982; Valentim et al. 1993). In addition, the analysis of three-dimensional (3D) facial changes could not be accomplished by 2D methods. Chen et al. (2012) developed a new way of individualized prediction of 3D facial soft tissue changes after orthodontic treatment based on the finite element method (FEM). However, patients' requests for facial esthetics are not confined to static facial profile, dynamic condition, i.e., smile esthetics is also a main concern. Gummy smile (Pithon et al. 2013; Rodríguez-Martínez et al. 2014) and dark triangular areas of buccal corridor (Roden-Johnson et al. 2005) during smiling are regarded as unattractive, patients wonder whether this kind of unattractive smile would happen or whether already existed unattractive smile could be improved after orthodontic treatment (Maganzini et al. 2014; Meyer et al. 2014), thus prediction of smiling expressions should be taken into account in orthodontic treatment planning.

Blend shape, simulation and performance-driven are the three major computer animation approaches that have been used for generation of facial dynamic expressions (Ersotelos and Dong 2008). Blend shape was used for generating synthetic expression from a set of existing example facial poses of one subject, where a considerably large model collection was needed (Li et al. 2010). Facial simulation was usually performed on the individualized anatomy-based craniofacial finite element model, where facial expression was driven by facial expression muscles, however, confirmation of muscle parameters was difficult and time-consuming (Beldie et al. 2010; Wu et al. 2013). Performance-driven approach was based on transferring of true dynamic expression acquired by motion capture equipment, which was thought to be easier, faster and more realistic. This approach was popularly used for reconstruction of dynamic expression (Guenter et al. 1998; Pighin et al. 1999), while only Noh and Neumann (2001) applied this approach to expression cloning through transferring the recorded dynamic expression to a different model. Since the post-treatment craniofacial model was different from the pre-treatment craniofacial model due to orthodontic related as well as growing or aging related dentoalveolar changes, the method proposed by Noh and Neumann (2001) was supposed to be more applicable for dynamic smile prediction after orthodontic treatment.

*Corresponding author. Email: elisa02chen@gmail.com; tmxuortho@gmail.com

Accurately acquisition of dynamic expression by motion capture equipment was an important premise for expression transfer. In Noh and Neumann's study (2001), it was recorded by tracking a number of landmark points and calculated as motion vectors of model vertices. A color-encoded structured light system invented by Chen et al. (2007) could acquire dynamic facial expression without landmark point labeling, which would be more convenient for clinical application.

With a combination of the color-encoded structured light system and cone beam computed tomogr (CBCT), this study investigated a new method for prediction of dynamic smiling expressions after orthodontic treatment based on expression transfer, in which dynamic smiling expressions were interpreted as a matrix of facial depth changes (Chen et al. 2008) and the accuracy of this method was evaluated.

2. Materials and methods

2.1. Subject

A 25-year-old female orthodontic patient without obvious facial deformity or smile disorder was enrolled. The orthodontic treatment plan included extraction of four first bicuspids, teeth aligning, maximum anchorage to retract the anterior teeth to alleviate lip prominence and vertical control of upper anterior teeth to avoid gummy smile. This study was reviewed and approved by the ethics committee of Peking University School and Hospital of Stomatology. The written informed consent was obtained from the participated patient.

2.2. Image acquisition and processing

Pre-treatment and post-treatment craniofacial CBCT images and 3D dynamic smiling expressions were acquired.

The craniofacial CBCT images were taken from the patient in rest jaw position and neutral expression, the scanning settings of the CBCT scanner (DCT Pro, Vatech Co., Yongin-Si, Korea) were as follows: 20 cm × 19 cm field of view (FOV), 90 kVp tube voltage, 7 mA tube current and 15 s scan time. The images were imported into Amira 5.2.2 (Visage Imaging Inc., CA, USA). 3D models of craniofacial hard tissue and soft tissue were reconstructed separately by threshold segmentation method. The reconstructed 3D models were further precisely processed with Geomagic Studio 12 (Raindrop Geomagic Inc., Morrisville, NC, USA), including trimming useless area, filling holes and smoothing. The final models are shown in Figure 1.

The dynamic smiling expressions were scanned with a 3D color-encoded structured light system, which consisted of a projector (EPSON EB-C301MN, Seiko Epson Inc., Tokyo, Japan), a CCD camera (CANON EOS 60D, Canon Inc., Tokyo, Japan) and a computer (Intel Core i5-3570K CPU, × 64, 8 GB RAM, Windows 8 system). The maximum image acquisition rate was six frames per second (FPS), and maximum video acquisition rate was 25 FPS. Details of this color-encoded structured light system could refer to Chen et al. (2007, 2008). The scans were reconstructed into a sequential of 3D facial surface point cloud, which were wrapped into triangular patches of geometrical models. These models were defined as dynamic smiling models (Figures 2 and 3).

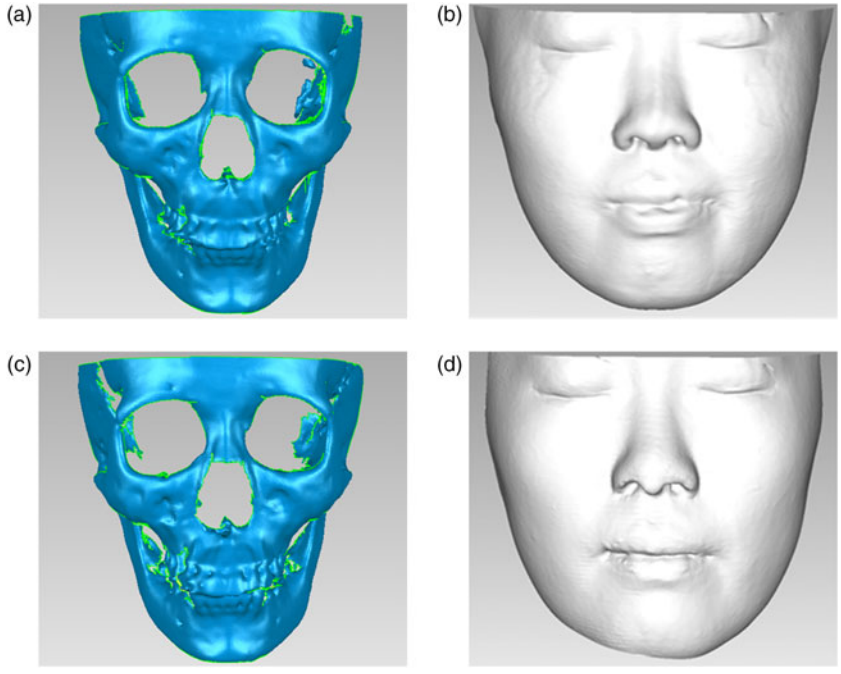

Figure 1. Pre-treatment (a) and post-treatment (b) models of craniofacial hard tissue and soft tissue from CBCT.

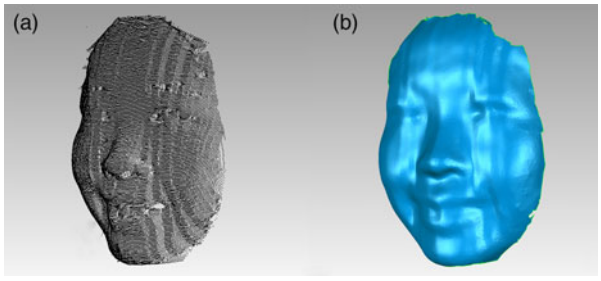

Figure 2. (a) 3D facial point cloud reconstructed from the color-encoded structured light system. (b) Dynamic facial smiling model generated from 3D point cloud.

2.3. Registration of 3D craniofacial models

In order to integrate all craniofacial image data of the subject, the sequential dynamic smiling models and the static CBCT models of hard tissue and soft tissue need to be registered in the same coordinate system. The registration included two parts: within the dynamic models to eliminate minor head movements which may happen during smiling and between dynamic model and static model which were reconstructed from different resources.

First, the dynamic models were registered on nasion, which was relatively stable during smiling expressions, with a combination of initial point registration and final regional registration based on iterative closest point algorithm. Then the static model of soft tissue was registered onto the first dynamic facial model (neutral expression) of the sequential smiling expressions (Figure 4), transformation matrix was calculated from the registration result. With application of the same transformation matrix, static model of hard tissue was also registered onto the dynamic model successfully.

Figure 3. Dynamic facial models of a sequential smilling expressions from the 3D color-encoded structured light system.

2.4. Calculation of facial depth changes of the sequential smiling expressions

The facial changes during smiling expressions could be interpreted as changes of facial depth from hard tissue surface to soft facial surface.

The method of measuring facial depth: for each triangular patch of the 3D model of hard tissue, the center of gravity was defined as original point, from which the normal vector extended outward and intersect with the 3D dynamic facial model, the distance from original point to intersection point was defined as facial depth (Figure 5).

Given that the model of hard tissue had n triangular patches, and the number of facial dynamic models was m. For $0 \le i \le n$ and $0 \le j \le m$, h_i^j was defined as the distance from the center of gravity of number i triangular patch to the corresponding intersection point of number j dynamic model. Thus, for number i triangular patch, a group of facial depth value could be obtained as h_i^0, $h_i^1, \ldots, h_i^m$, and facial depth change $d_i^j = h_i^j - h_i^0$, ultimately, a matrix of facial depth changes for the whole model was obtained as

$$D = \begin{bmatrix} d_1^1 & d_1^2 & \cdots & d_1^m \\ d_2^1 & d_2^2 & \cdots & d_2^m \\ \vdots & \vdots & \ddots & \vdots \\ d_n^1 & d_n^2 & \cdots & d_n^m \end{bmatrix}. \quad (1)$$

The facial depth changes during smiling are shown in Figure 6.

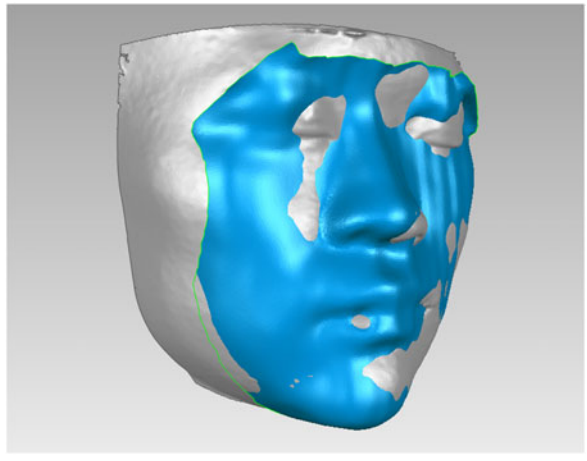

Figure 4. Registration of static model of soft tissue and the first dynamic facial model (neutral expression) of the sequential smiling expressions. Gray: static model of soft tissue from CBCT. Blue: facial dynamic model from color-encoded structured light system.

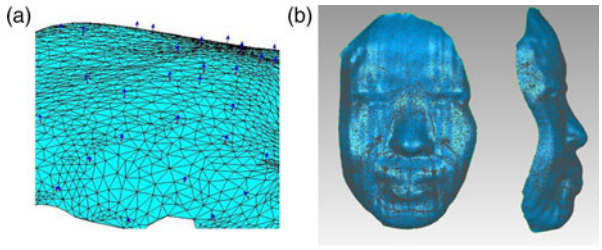

Figure 5. (a) Blue arrows indicated outer normal vectors from the center of gravity of triangular patches of the 3D model of hard tissue. (b) Black points indicated intersection points on the 3D dynamic facial model.

2.5. Smile transfer and accuracy verification

Since the matrix of 3D facial depth changes during smiling was obtained, smile transfer could be realized by applying the matrix to any other craniofacial model. To evaluate the accuracy of smile transfer, the matrix of facial depth changes was applied to the same static model of pre-treatment to produce animated smiling expressions. Shell-to-shell deviation between the models of real scanned smiling expression and animated smiling expression was calculated as the error of smile transfer.

2.6. Smile prediction and accuracy verification

Our hypothesis was that the smiling pattern would remain unchanged for the same pre- and post-treatment subject, thus smile prediction could be achieved through transference of pre-treatment smiling expressions to the predicted static craniofacial model of post-treatment. To evaluate the accuracy of smile prediction, post-treatment craniofacial models, including the static model from CBCT and dynamic smiling models from the color-encoded structured light system were collected in the selected subject.

The static models of pre- and post-treatment were registered in the nose and forehead area which would not be affected by orthodontic treatment, the treatment changes of hard tissue mainly occurred on the upper and lower teeth as well as surrounding alveolar bone, the static model of soft tissue also changed accordingly with less protrusive lips (Figure 7).

For applying the matrix of facial depth changes to the model of post-treatment, triangular meshes of pre- and post-treatment models of hard tissue must be matched first. Given the triangular mesh of pre-treatment model is

$$\{V_s, F_s\} = \left\{V_{s_1}, V_{s_2}, \ldots, V_{s_n}, F_{s_1}, F_{s_2}, \ldots, F_{s_m}\right\} \quad (2)$$

and that of post-treatment model is

$$\{V_t, F_t\} = \left\{V_{t_1}, V_{t_2}, \ldots, V_{t_q}, F_{t_1}, F_{t_2}, \ldots, F_{t_p}\right\}, \quad (3)$$

where V denoted the vertex and F denoted the triangular facet, the triangular mesh of pre-treatment model had n vertices and m triangular facets, and that of post-treatment

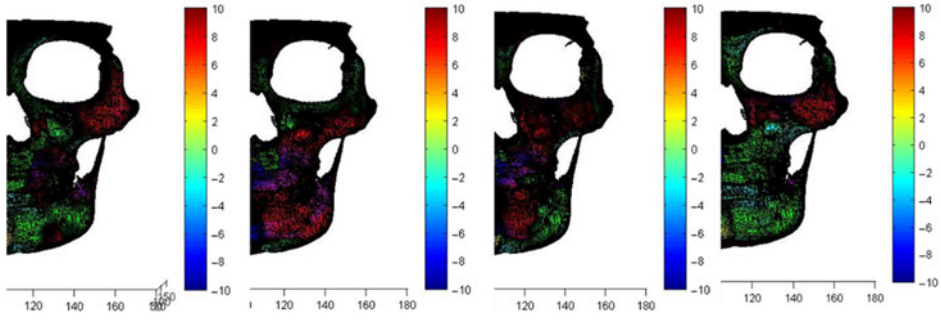

Figure 6. Color maps showed the facial depth changes during smiling. Note: Only half of face was calculated to simplify.

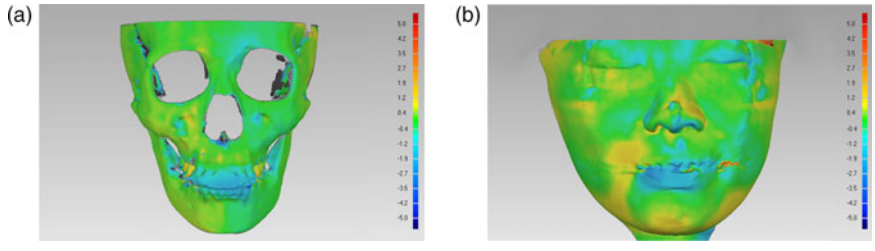

Figure 7. (a) Shell-to-shell deviations between pre-treatment and post-treatment models of hard tissue, it showed dentoalveolar retraction by about 2 mm after orthodontic treatment. (b) Shell-to-shell deviations between pre-treatment and post-treatment models of soft tissue, it showed a decrease of lip protrusion by about 1–2 mm.

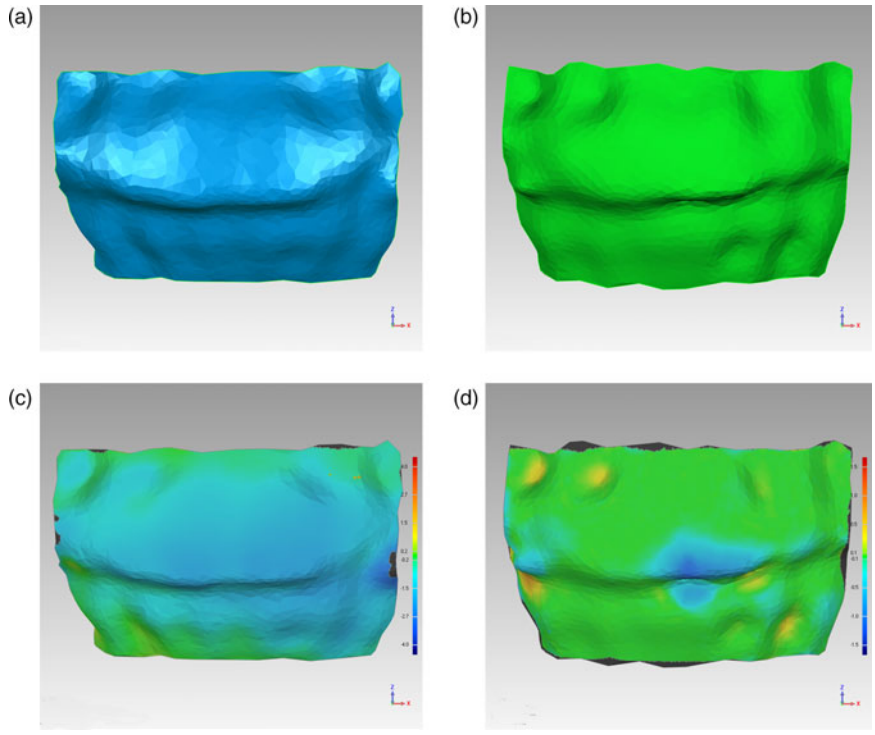

Figure 8. Matching of triangular meshes between pre- and post-treatment models in the dentoalveolar region. (a) Pre-treatment dentoalveolar region was indicated by blue color. (b) Post-treatment dentoalveolar region was indicated by green color. (c) Registration of pre- and post-treatment dentoalveolar region, big deviation indicated obvious orthodontic change. (d) Registration of post-treatment dentoalveolar regions before and after matching of triangular meshes, small deviation indicated good matching.

model had q vertices and p triangular facets, a new group of vertices

$$\{V'_s\} = \left\{V'_{s_1}, V'_{s_2}, \ldots, V'_{s_n}\right\} \tag{4}$$

was solved out by radial basis function (Seol et al. 2011), making that triangular mesh of $\{V'_s, F_s\}$ matched with that of $\{V_t, F_t\}$. To simplify the calculation, only dentoalveolar region undergoing orthodontic treatment changes did the matching process (Figure 8), the rest craniofacial areas still used for the pre-treatment model.

With the matched post-treatment model of hard tissue, corresponding intersection points in the post-treatment model of soft tissue were located using the same method described in Section 2.4. Then the matrix of facial depth changes of pre-treatment smiling expressions was applied to these intersection points to generate the predicted smiling expressions on the post-treatment static soft tissue model. This predicted smiling result was compared with the real scanned one post-treatment and shell-to-shell deviation was displayed to evaluate the accuracy of smile prediction.

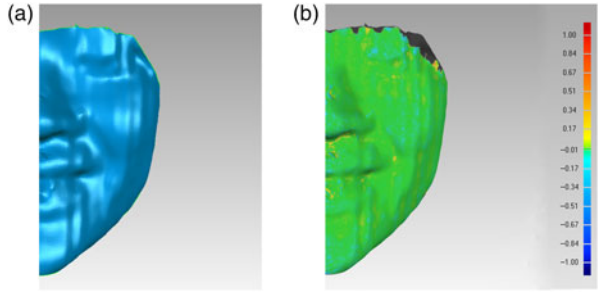

Figure 9. (a) Animated smiling model through smile transfer to the original pre-treatment static model. (b) Shell-to-shell deviation between the animated and real scanned smiling model of pre-treatment. Small deviation within 0.05 mm indicated accurate smile transfer. Note: Only half of face was calculated to simplify.

3. Results

3.1. *Smile transfer and accuracy verification*

Figure 9 showed the shell-to-shell deviation between the animated and real scanned smiling model of pre-treatment. Most area displayed green color that indicated an error within ± 0.01 mm, the positive and negative mean values of error were 0.01 and -0.02 mm respectively, with the standard deviation of ± 0.03 mm.

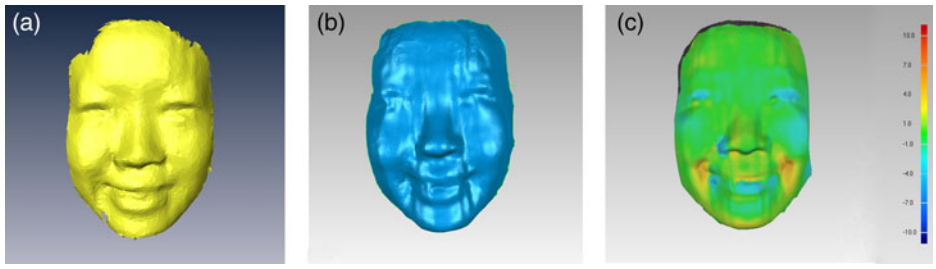

Figure 10. (a) Real scanned smiling model of post-treatment. (b) Predicted smiling model through smile transfer to the post-treatment static model. (c) Shell-to-shell deviation between the predicted and real scanned smiling model of post-treatment. The positive and negative mean values of error were 0.9 and −1.1 mm respectively, with the standard deviation of ±1.5 mm.

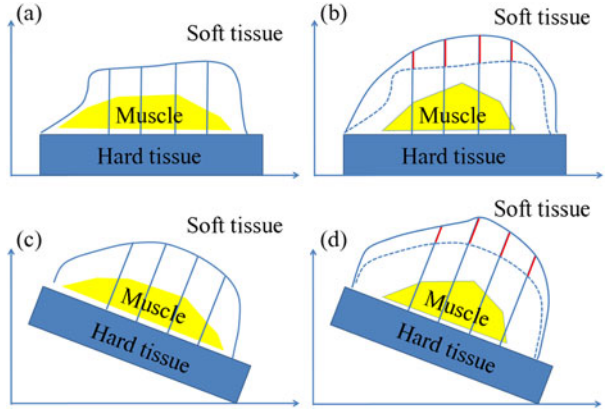

Figure 11. The diagram of the principle of smile prediction. (a) Static craniofacial model with neutral expression, blue straight lines indicated facial depth from surface of hard tissue to surface of soft tissue. (b) Solid curve indicated surface of soft tissue with smiling expression, dotted curve indicated surface of soft tissue with neutral expression, red straight lines indicated facial depth changes due to smiling. (c) Hard tissue of the craniofacial model changed in shape or position. (d) Based on the assumption that smiling pattern of the same subject did not change after orthodontic treatment, the facial depth changes indicated by red straight lines remained the same regardless of hard tissue change.

3.2. *Smile prediction and accuracy verification*

Figure 10 showed the shell-to-shell deviation between the predicted and the real scanned smiling model of post-treatment. The positive and negative mean values of error were 0.9 and −1.1 mm respectively, with the standard deviation of ±1.5 mm. The maximum deviation existed in the perioral area, indicated by orange and cyan color, close to ±4.0 mm.

4. Discussion

This study proposed a new way of individualized facial expression transfer for the purpose of dynamic smile prediction in orthodontic treatment planning. Consecutive dynamic facial smiling expressions were obtained through a 3D color-encoded structured light system at a maximum speed of six FPS. Time-consuming feature landmarks location (Noh and Neumann 2001) was not needed. The whole time taken for generation of a smile prediction model consisting of 59,863 vertices was about 10 min, including 681 s for reconstruction of 3D point cloud from the scanning data, 393 s for solving out the intersection points on the facial soft tissue model with a hard tissue model consisting of 18,000 triangles and only 0.2 s for calculation of the matrix of facial depth changes. Compared with the traditional physical-based FEM for expression simulation, which took about 2 h for a model consisting of 500 vertices (Wu et al. 2013), the novel efficient method in this study would be more applicable for clinical use.

This method of smile prediction was based on the assumption that smiling pattern did not change for the same subject pre- and post-orthodontic treatment. Though dentoalveolar hard tissue would change after orthodontic treatment, the defined facial depth changes resulted from constriction of facial expression muscles when smiling was supposed to be the same. Thus post-treatment smile could be predicted through adding the facial depth changes to the post-treatment static model. The diagram of the principle of smile prediction was illustrated in Figure 11. The accuracy of smile transfer for the pre-treatment model was within 0.05 mm, and the accuracy of smile prediction for the post-treatment model was +0.9/−1.1 mm, with the maximum error of ±4.0 mm in perioral areas. This area corresponded to the dentoalveolar region of orthodontic treatment change; therefore, accurate reconstruction of this region would decrease the error of smile prediction. Integration of precise teeth crowns from 3D digital dental cast or directly from intraoral digital scanning into the static models could be helpful. Besides, for the real subject, even the smiling pattern generally remained the same, there still might be slight difference between the pre- and post-treatment smiling expressions.

In our previous study for the prediction of static facial soft tissue model based on FEM (Chen et al. 2012), the mean error was +0.85/−1.05 mm and maximum error was +5.5/−6.2 mm, the error of dynamic smile prediction was within the range of error of static facial soft tissue prediction. Further studies would be conducted to reduce

the prediction error from both the static and dynamic sides as well as to explore automatically combined prediction from the two sides. Besides, tracing the contours of lip to elucidate its accurate relationship with teeth should be supplemented for smile esthetic evaluation.

5. Conclusions

This study proposed a new way of individualized facial expression transfer for the purpose of dynamic smile prediction in orthodontic treatment planning. 3D craniofacial data from CBCT and color-encoded structured light system were combined to construct a prediction model, in which dynamic facial expression was interpreted as a matrix of facial depth changes. These data, which extracted from the pre-treatment smile expression record, were applied to the post-treatment static model to realize expression transfer. Therefore smile esthetic of the patient after treatment could be evaluated in pre-treatment planning procedure. The accuracy was clinically acceptable. Further study of smile transfer to the predicted post-treatment static model would be implemented for future clinical use.

Acknowledgements

The authors are grateful to the Center for BioMed-X Research, Academy for Advanced Interdisciplinary Studies, Peking University, for providing the 3D color-encoded structured light system.

Conflict of interest disclosure statement

No potential conflict of interest was reported by the authors.

Funding

This work is supported by the National Natural Science Foundation of China [grant number 81200806] and [grant number 81371192].

References

Beldie L, Walker B, Lu Y, Richmond S, Middleton J. 2010. Finite element modelling of maxillofacial surgery and facial expressions – a preliminary study. The International Journal of Medical Robotics and Computer Assisted Surgery. 6(4):422–430. doi:10.1002/rcs.352.

Chen S, Lou H, Guo L, Rong Q, Liu Y, Xu TM. 2012. 3-D finite element modelling of facial soft tissue and preliminary application in orthodontics. Computer Methods in Biomechanics and Biomedical Engineering. 15(3):255–261. doi:10.1080/10255842.2010.522188.

Chen HJ, Zhang J, Fang J. 2008. Surface height retrieval based on fringe shifting of color-encoded structured light pattern. Optics Letters. 33(16):1801–1803. doi:10.1364/OL.33.001801.

Chen HJ, Zhang J, Lv DJ, Fang J. 2007. 3-D shape measurement by composite pattern projection and hybrid processing. Optics Express. 15(19):12318–12330. doi:10.1364/OE.15.012318.

Ersotelos N, Dong F. 2008. Building highly realistic facial modeling and animation: a survey. The Visual Computer. 24(1):13–30. doi:10.1007/s00371-007-0175-y.

Guenter B, Grimm C, Wood D, Malvar H, Pighin F. 1998. Making faces. Proceedings of the 25th Annual Conference on Computer Graphics and Interactive Techniques, ACM.

Hillesund E, Fjeld D, Zachrisson BU. 1978. Reliability of soft-tissue profile in cephalometrics. American Journal of Orthodontics. 74(5):537–550. doi:10.1016/0002-9416(78)90029-5.

Li H, Weise T, Pauly M. 2010. Example-based facial rigging. ACM Transactions on Graphics (TOG). 29:32.

Maganzini AL, Schroetter SB, Freeman K. 2014. Improvement in smile esthetics following orthodontic treatment: a retrospective study utilizing standardized smile analysis. The Angle Orthodontist. 84(3):492–499. doi:10.2319/072913-564.1.

Meyer AH, Woods MG, Manton DJ. 2014. Maxillary arch width and buccal corridor changes with orthodontic treatment. Part 2: attractiveness of the frontal facial smile in extraction and nonextraction outcomes. American Journal of Orthodontics and Dentofacial Orthopedics. 145(3):296–304. doi:10.1016/j.ajodo.2013.10.019.

Noh JY, Neumann U. 2001. Expression cloning. Proceedings of the 28th Annual Conference on Computer Graphics and Interactive Techniques, ACM.

Pighin F, Szeliski R, Salesin DH. 1999. Resynthesizing facial animation through 3D model-based tracking. Computer vision, 1999. The Proceedings of the Seventh IEEE International Conference; 1999 Sep 20–27; Kerkyra.

Pithon MM, Santos AM, Viana de Andrade ACD, Santos EM, Couto FS, da Silva Coqueiro R. 2013. Perception of the esthetic impact of gingival smile on laypersons, dental professionals, and dental students. Oral Surgery, Oral Medicine, Oral Pathology and Oral Radiology. 115(4):448–454. doi:10.1016/j.oooo.2012.04.027.

Roden-Johnson D, Gallerano R, English J. 2005. The effects of buccal corridor spaces and arch form on smile esthetics. American Journal of Orthodontics and Dentofacial Orthopedics. 127(3):343–350. doi:10.1016/j.ajodo.2004.02.013.

Rodríguez-Martínez A, Vicente-Hernández A, Bravo-González LA. 2014. Effect of posterior gingival smile on the perception of smile esthetics. Medicina Oral, Patologia Oral y Cirugiabucal. 19:e82.

Roos N. 1977. Soft-tissue profile changes in Class II treatment. American Journal of Orthodontics. 72(2):165–175. doi:10.1016/0002-9416(77)90057-4.

Seol Y, Seo J, Kim PH, Lewis JP, Noh J. 2011. Artist friendly facial animation retargeting. ACM Transactions on Graphics (TOG). 30(6):162. doi:10.1145/2024156.2014196.

Valentim ZL, Capelli JJ, Almeida MA, Bailey LJ. 1993. Incisor retraction and profile changes in adult patients. The International Journal of Adult Orthodontics and Orthognathic Surgery. 9:31–36.

Waldman BH. 1982. Change in lip contour with maxillary incisor retraction. The Angle Orthodontist. 52:129–134.

Wu T, Hunter P, Mithraratne K. 2013. Simulating and validating facial expressions using an anatomically accurate biomechanical model derived from MRI data. Proceedings of the International Conference on Computer Graphics Theory and Applications and International Conference on Information Visualization Theory and Applications; Setubal, Portugal.